

CHAPTER – 6

GROUND PENETRATING RADAR STUDIES

The use of Ground Penetrating Radar (GPR) as a tool for geological investigation continues to expand in scope and applications. This high-resolution GPR technique has proved to be particularly useful in sedimentary geology and geomorphology because it is a nondestructive geophysical method effective in imaging the shallow subsurface (Hickin et al., 2007). GPR technique is widely used to precisely delineate and map active fault and identify tectonic deformation, earthquake-induced surface ruptures and other related secondary deformation features such as liquefaction craters (Maurya et al., 2006; Patidar et al., 2007; 2008). GPR has been shown to successfully investigate the geological properties of the shallow subsurface by detecting changes in the physical character of the subsurface commonly associated with geological features in the form of radar reflections caused by contrasts in the dielectric properties of adjacent materials (Davis and Annan, 1989; Busby and Merritt, 1999; Gross et al., 2002; Rashed et al., 2003; Maurya et al., 2005; 2006; Patidar et al., 2007; 2008). It is done by generation, transmission, propagation, reflection and reception of high frequency electromagnetic energy pulses (Neal, 2004). The depth of the GPR survey is dependent on the antenna frequency; the higher the antenna frequency, the shallower the depth of penetration (Neal, 2004). A detailed description of the fundamentals and working principles of GPR can be found in (Davis and Annan, 1989; Smith and Jol, 1995; Annan, 1996; Maurya et al., 2005; Patidar et al., 2006).

Location of transects for GPR studies carried out are shown in Figure 5.2. All GPR profiles presented here were acquired by dragging the 200 MHz antenna along transects selected after geomorphic studies. Knowledge of the geomorphic and the geological settings guided us to select the input parameters required for data acquisition. A good radar data quality with minimal noise levels was obtained as all transects selected were free of substantial vegetation and located far away from anthropogenic influences. Post-survey processing of raw GPR data follows the basic principles of seismic data processing and is mainly aimed at removal of noise without comprising the original data (Aksu et al., 2017). The sequential steps followed during processing of GPR data are elaborated in Chapter – 3. The processed and interpreted GPR profiles are shown in Figures 6.2 to 6.7.

Interpretation of GPR profiles is based on groups or sets of reflectors based on their characteristics and parameters including amplitude pattern and reflection geometry in the

subsurface (Davis and Annan, 1989; Smith and Jol, 1995; Maurya et al., 2005; 2017a; Patidar et al., 2007; 2008; 2010). Extensive GPR studies carried in Quaternary deposits in various sedimentary environments demonstrate that identifying distinct sets of reflectors with similar characteristics and identifying them as radar facies is very advantageous in interpreting the nature of subsurface sediment fill (Jol et al., 1996; Overmeeren, 1998; Vandenberghe and Overmeeren, 1999; Pellicer and Gibson, 2011; Zarroca et al., 2017; Mertes et al., 2017). In the GPR data, recognizing the miliolite deposits in the subsurface was relatively simpler as these deposits showed good returns while the Mesozoic rocks yielded poor returns due to attenuation of radar waves (Figures 6.2 to 6.7). The internal sedimentary architecture of the miliolites is interpreted on the basis of various radar facies using reflector characteristics. A total of eight radar facies has been identified (Table 6.1). The details regarding the acquisition and utilisation of the velocity data during the processing of the profiles is described are described below.

Velocity data was obtained by common mid-point (CMP) surveys carried out using 40 MHz antenna to estimate the propagation velocity of Electro-Magnetic (EM) waves in the subsurface (Figure 6.1).

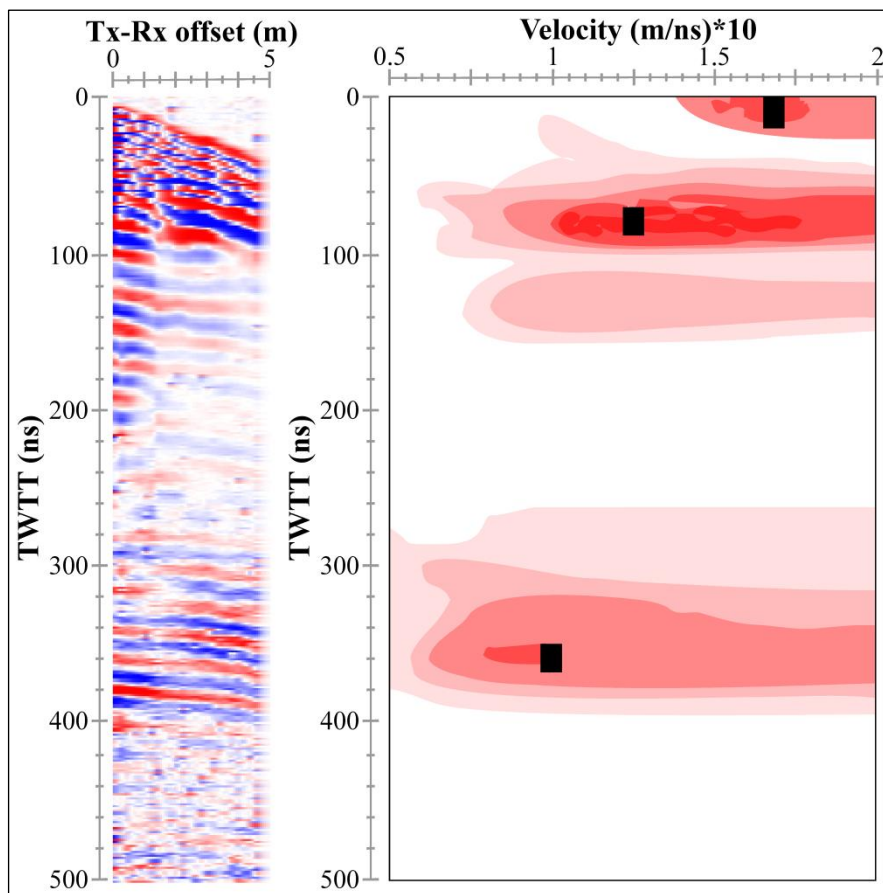


Figure 6.1 CMP radargram recorded using 40 MHz bi-static antenna configuration. Derived semblance plot is shown on the right side.

Table 6.1 Details of the observed radar facies and their geological interpretation. Radar facies nomenclature is based on amplitude response, continuity and geometry of reflectors.

Radar facies	Radar response characteristics	Geological interpretation
Rf1	Marks the top of radargrams; long and consistent; horizontal to sub horizontal reflectors of high-amplitude sloping towards valley centre; internal bounding surfaces typically absent	Sediments washed down in phases along the hilly slopes forming the valley sides; found only in buried paleovalley and wind gap
Rf2	High-amplitude, sub-parallel, inclined reflections with moderate to high dip (5°–60°); reflections are continuous and show good lateral consistency. Reflections are straight to curved or concave-up; internal bounding surfaces indicated by relatively strong internal reflectors.	Foresets of intermediate to large scale aeolian cross stratification in miliolite sediments deposited in the bedrock river valley; most abundant with offset and steepening of foresets along fault in miliolite deposits overlying KHF
Rf3	Moderate- to high-amplitude, parallel to sub-parallel, semi-continuous, wavy reflections with <7° dip; most widespread and laterally consistent in paleovalley; occasionally internal reflections downlap onto the lower erosional truncation surfaces; internal bounding surfaces occasional	Partially reworked aeolian miliolite deposits; prograding wedges extending towards valley centre with primary inclined bedding; occasional internal bounding surfaces possibly correlate with remnant parts aeolian miliolites
Rf4	Low- to moderate amplitude, semi-continuous, overlapping wedges and occasionally chaotic reflection pattern. The reflectors form trough-shaped geometry with 35–40° dip. The erosional base of the convoluted troughs shows well-defined reflections. No internal bounding surface. Multiple trough fills are found. The internal reflections show variety of trough fill patterns – semi-continuous to chaotic, wavy to convoluted, convergent	Fluvially reworked miliolite deposits; trough shaped cut and fill structures; occasional chaotic reflectors attributed to coarse clasts of bedrock incorporated in miliolite deposits
Rf5	Low-amplitude and semi-continuous reflections; highly deformed reflections in deposits overlying KHF; no internal bounding surface	Fluvially reworked miliolite sediments with coarse clasts/debris; found to be offset and deformed in deposits overlying KHF indicating post-miliolite surface faulting
Rf6	Moderate- to high-amplitude, horizontal to sub-horizontal, parallel to sub-parallel,	Fairly well stratified reworked miliolite deposits

	semi-continuous, wavy reflections. Well-defined internal bounding surfaces.	
Rf7	Low-amplitude, broken, chaotic reflector patterns with moderate to poor continuity; lack of bounding surfaces	Basal gravelly deposits at the bottom of paleovalley sediment fill; comprising poorly sorted gravelly fluvial miliolite deposits.
Rf8	Low amplitude reflectors with poor continuity; forming zone of high attenuation of radar waves	Well lithified bedrock comprising Mesozoic formations

The data was recorded at multiple offsets using bi-static antennae configuration. At first, the transmitting and receiving antennas are begun to operate at zero-offset position (1 m). Data were then collected at multiple offsets by moving apart both the antennas from the zero-offset position with the step size of 10 cm. CMP data were collected up to the total offset of 5 m horizontal distance (Figure 6.1). Through CMP profile analysis, the estimated average velocity of 0.4 m ns^{-1} is derived from the semblance plot, corresponding to a dielectric constant of 5. This value has been used for time to depth conversion of all the collected GPR profiles described below.

GPR CHARACTERISATION OF QUATERNARY SEDIMENTS

The Late Quaternary sediments in the Katrol Hill Range comprise dominantly aeolian and fluvial miliolites, alluvium and colluvial sediments. Most of the depressions, river valleys and the base of north facing KHF scarps and overlapping the fault zone show aeolian or partially reworked miliolites. In the present study, most of the GPR transects covered miliolite outcrops for radar characterization of sediments and sediments overlapping the fault line to decipher signatures of faulting in Late Quaternary sediments.

Transect 1 – Wind gap in Katrol Hill Range

The GPR survey was carried out to image the subsurface architectural setup of the morphology of the wind gap in the Gangeshwar basin in Katrol Hill Range (indicated as T1 in Figure 5.2) and to differentiate various depositional units in the miliolite deposits. This transect (Figure 6.2) is oriented in the E-W direction, which is across the almost flat depositional surface of the north trending miliolite filled wind gap described above. A 125–180 ns penetration depth was found sufficient to locate the major bounding surfaces, to detect the depth to bedrock and to study the characteristics of sediment fill in the wind gap. Figure 6.2a, b, c shows the 87 m long processed and interpreted GPR profile acquired across the wind gap.

Erosional truncation surfaces are identified on the basis of abrupt termination of distinct sets of radar facies/reflectors above and below it (Figure 6.2b). These surfaces can be short to long and of consistent continuity. Two such distinct surfaces are indicated in the GPR profile along Transect 1 (T1) in Figure 6.2b. Both erosional surfaces are consistently traceable through the profile. The morphology of the lower surface suggests that it marks the buried bedrock valley profile. This surface shows sharp truncation of low amplitude chaotic reflections of the Mesozoic rocks below with the high amplitude consistent reflectors of varying characteristics above forming the overlying sediment fill comprising miliolite deposits. The GPR data suggests that the morphology of the channel resembled a shallow, meandering bedrock river confined between the valley slopes consisting of hard and compact Mesozoic rocks. This inference is consistent with the presence of broad valleys in Mesozoic rocks in pre-miliolite time as suggested by Patidar et al. (2007).

The upper erosional truncation surface comprises a horizontal surface at 3-4 m depth below the surface of a paleo-valley (Figure 6.2c). This surface separates the overlying horizontal and sub horizontal reflectors (Rf1) and the underlying reflectors that show highly variable characteristics and comprising various other radar facies (Figure 6.2c). The overlying reflectors show downlapping characteristics while the reflectors below the truncation surface show onlapping characteristics, which correspond to channel fill deposits.

The top of the sediment fill is characterized by large, consistent, sub-horizontal and downlapping reflectors overlying the erosional truncation surface. These are interpreted as repeating deposits mainly from the valley sides on to the slope of the miliolite filled wind gap (Figure 6.2c). These sediments are interpreted as dominantly slope controlled deposition after the river activity had ceased as indicated by the underlying erosional truncation surface. Below this surface, a wide variety of radar facies (Rf2 to Rf7) are vertically stacked that fill the bed-rock valley completely (Figure 6.2c). Rf2 facies consists of high amplitude inclined reflections that are indicative of foresets of wind deposited miliolite sediments in the wind gap. These inclined reflectors broadly correlate with the slope of the valley walls. Similar reflection pattern that are relatively larger and wavy represent aeolian miliolites that are partially reworked by fluvial activity of the river flowing through the wind gap. Widespread occurrence of this facies in the wind gap suggests that though the river valley was almost overwhelmed by phases of aeolian miliolite deposition, the river continued to flow, as reflected by the weak fluvial activity (Figure 6.2c). The strongly ephemeral character of the river at this time confirms to the location of the area in hyper-arid climatic zone. Repeated

levels of erosional contacts between adjacent depositional units suggest episodic reworking of miliolite sediments by an ephemeral stream with seasonal flows.

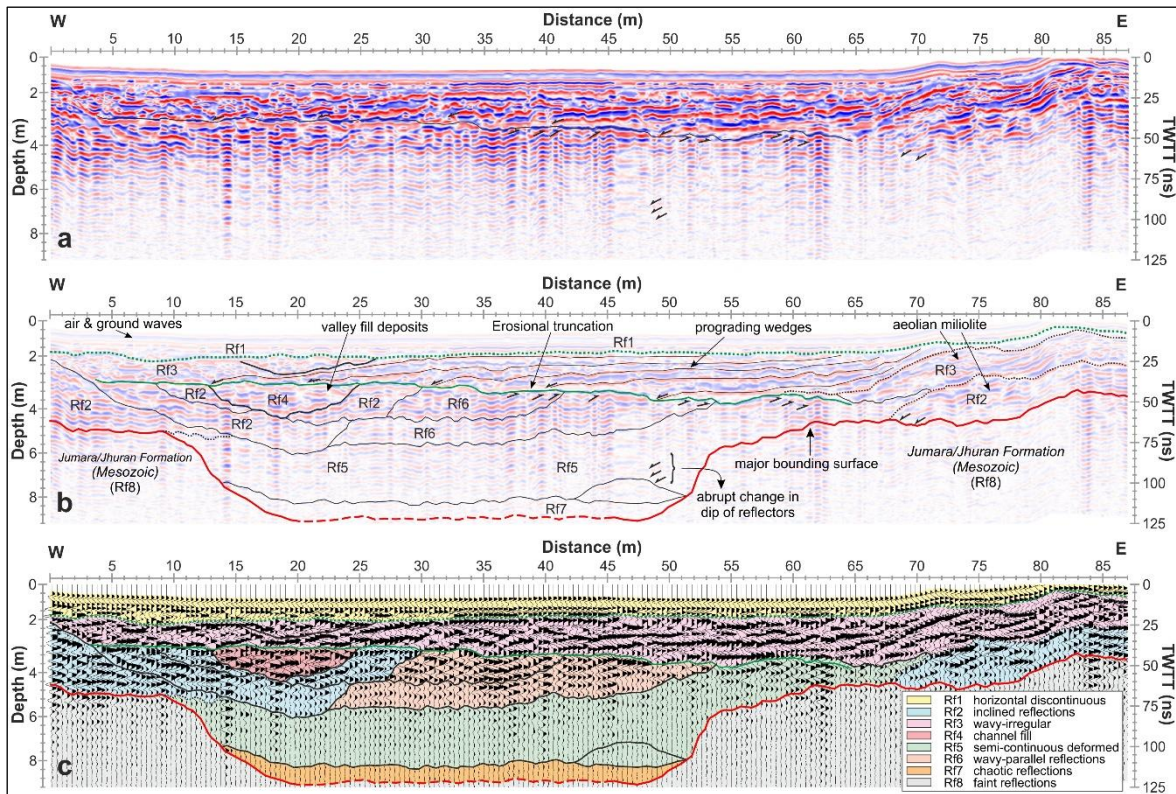


Figure 6.2 a. Processed GPR profile across the wind gap acquired using 200 MHz shielded antenna. Colour variation is a function of amplitude of radar waves in the subsurface. **b.** Processed GPR profile showing various radar facies. The radar facies are described in Table 6.1. **c.** Interpreted GPR profile in wiggle format. Axis on left side shows penetration depth in meters and on right side two-way travel time (TWTT) in ns is denoted. The upper axis shows the length of profile in meters. Note the broad bedrock valley filled with aeolian and reworked Late Quaternary miliolite sediments. The reworked miliolites are attributed to the paleo-Gangeshwar river that flowed northward through the wind gap. The prominent erosional truncation surface closer to the surface marks the end of fluvial activity in the channel indicating loss of catchment of the paleo-Gangeshwar river due to river diversion induced by tectonic tilting as explained in the text. The major bounding surface of wind gap is highlighted by thick red lines in Figures b and c. Note that at the base, the sediment-bedrock interface is poorly defined, marked by red dashed line. The erosional truncation surface is denoted by green continuous line, conformable contact in between the Quaternary deposits is marked by green dotted line and internal bounding surfaces in between the radar facies are marked by black continuous/dotted lines in Figures b and c.

Parts of the sediment fill changes low to moderate amplitude, onlapping and occasionally chaotic reflections (Rf5) suggest miliolite deposits reworked by fluvial action (Figure 6.2c). Chaotic reflectors are caused by pebbles and cobbles of Mesozoic rocks, which is a normal characteristic of fluvial miliolites (Patidar et al., 2007). Trough shaped

cut and fill structures in this radar facies provide further evidence that the river continued to flow northward and further through the wind gap during the phase of miliolite deposition. In the lower part of the sediment fill, the horizontal to sub-horizontal, semi-continuous to wavy reflections (Rf6) indicate well-stratified reworked miliolite deposits (Figure 6.2c). The Rf7 facies at the bottom of the sediment fill is characterized by a low amplitude, chaotic reflection pattern and interpreted as the basal gravelly unit with poor sorting (Figure 6.2c).

Transect 2 – Buried paleo-valley in Katrol Hill Range

This transect (indicated as T2 in Figure 5.2) is located on the left bank of Gangeshwar river that flows northward. The river at this location takes an eastward swing for a short distance before continuing to flow northwards. The 57 m long transect (Figure 6.3) was oriented perpendicular to the river bank at the location to image the variation in thickness and sedimentary facies. The GPR image along this transect provides data from the aeolian miliolites exposed along the valley slope to reworked miliolite deposits exposed in the incised river cliffs along the narrow channel of the Gangeshwar river in the centre of the paleo-valley (Figure 6.3a, b, c). The internal reflection characteristics of the various radar facies is described below.

Two distinct erosional truncation surfaces are observed (Figure 6.3b), similar to the ones identified along Transect 1. The lower southward sloping prominent truncation plane (Figure 6.3b) corresponds to the interface between the Mesozoic bedrock at the base and the overlying miliolite sediments. This plane separates the highly attenuated chaotic reflections (Rf8) below and the consistent reflections of high amplitude comprising the Rf5 and Rf7 radar facies (Figure 6.3c).

The eroded paleo-topography developed over Mesozoic rocks represents the pre-existing fluvial valley, which was later filled by aeolian and reworked miliolite deposits. The second truncation surface is seen in the uppermost part of the profile in Figure 6.3b. This runs consistently along the transect at a depth of ~1 m below the surface and separates the underlying high amplitude reflectors of varying characteristics representing miliolite deposits with the almost horizontal reflectors above. These reflectors sandwiched between the truncation surface and air and ground waves indicates surface soil with some slopewash sediments (Figure 6.3b). The upper truncation surface therefore marks the cessation of depositional phase of miliolite through aeolian and fluvial action. Another erosional truncation surface that is smaller extent than the above two surfaces, is also observed in the

GPR profile, shown as dotted line in Figure 6.3b. This surface is expected to continue beyond the GPR transect laterally towards the centre of the paleo-valley.

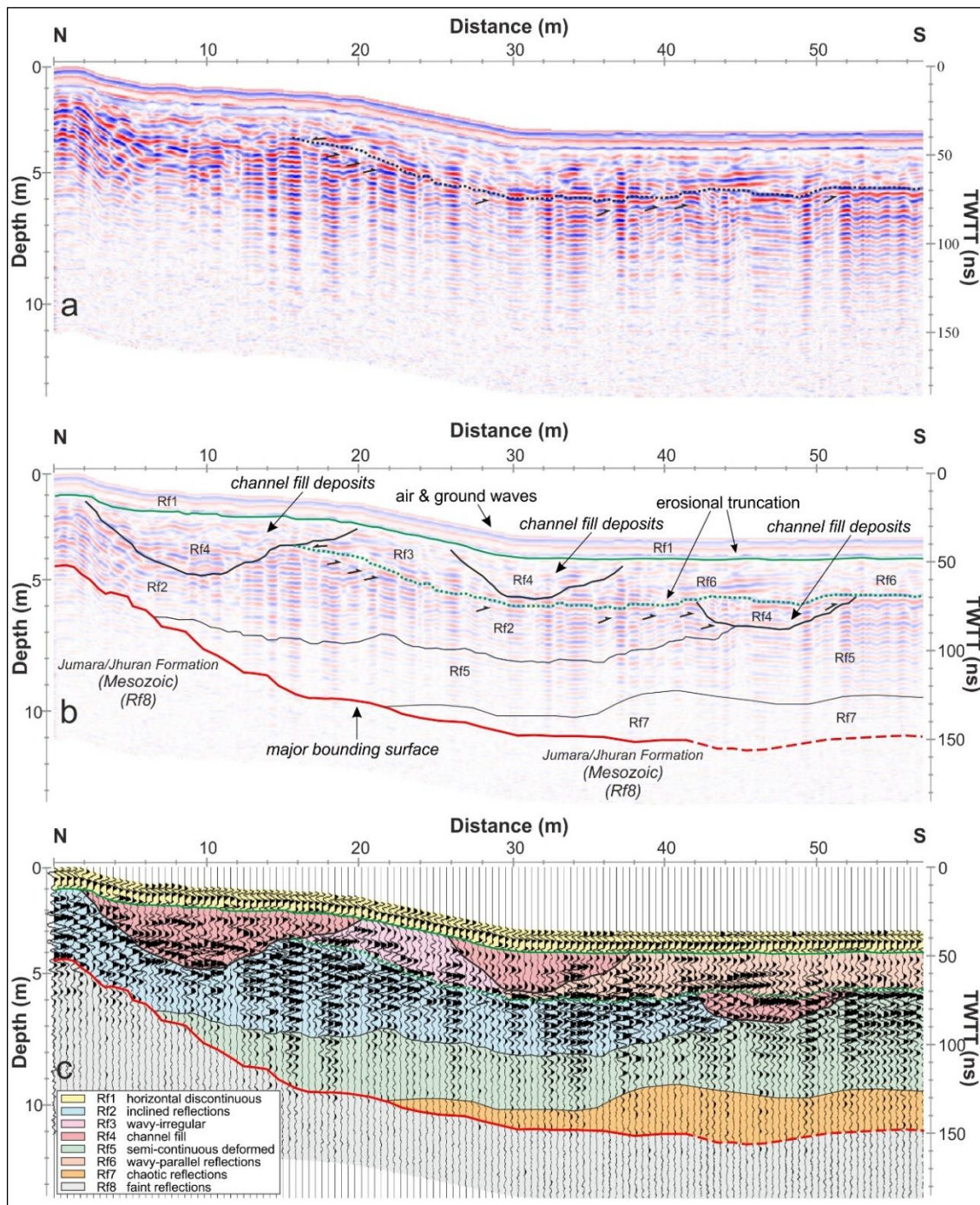


Figure 6.3 a. Processed GPR profile across the right bank of Gangeshwar river located in the buried paleo-valley acquired using 200 MHz shielded antenna. Color variation is a function of amplitude of radar waves in the subsurface. **b.** Processed radargram showing various radar facies. The radar facies are described in Table 6.1. **c.** Interpreted GPR profile in wiggle format. Note the sloping bedrock valley filled with aeolian and reworked Late Quaternary miliolite sediments. The prominent erosional truncation surface closer to the surface marks the end of fluvial reworking of miliolite sediments indicating due to river diversion after the depositional phase of miliolites. Follow Figure 6.2 caption for interpretation of radargrams.

This surface occurs at ~5 m below the surface is located within the sediment fill consisting of miliolite deposits and separates the Rf2 and Rf5 radar facies (Figure 6.3c) below and the overlying other facies containing channel troughs. The surface is found to abut against the largest one of these channel troughs. This erosional truncation is interpreted surface as a relatively short-lived hiatus, which was followed by resumption of fluvial activities by the river.

The reflectors between the two prominent erosional surfaces represent the sediment fill of the wind gap, which was deposited during the phase of miliolite deposition. Various radar facies identified (Rf2 to Rf7) comprise the vertically stacked miliolite sediments deposited by aeolian and fluvial processes (Figure 6.3c). Inclined, parallel to sub parallel reflectors of high amplitude represent miliolites with sets of aeolian cross stratification. In general, the inclination of the reflectors is similar to the valley slope indicated by the bottom erosional truncation surface suggesting deposition of miliolite sediments as obstacle dunes against the sloping rocky walls of the paleo-valley. Internal bounding surfaces indicate episodic aeolian sedimentation. Rf3 radar facies corresponds to partially reworked aeolian miliolites and is identified based on similarity in nature of reflectors as seen in the GPR data of Transect 1 (Figure 6.2c). Semi-continuous, occasionally chaotic and low to moderate amplitude reflection suggest the presence of cut and fill sediment troughs and channel fill. Three such troughs are observed in the hiatus upper parts of the GPR profile, of which, two are located above the minor erosional truncation surface marking a in Figure 6.3c. Rf6 comprise horizontal to sub horizontal reflectors with good consistency indicating the well-stratified nature of the reworked miliolite deposits. Rf7 comprises mostly discontinuous and chaotic reflectors suggesting a coarse gravelly nature of the basal part of the miliolite sediment fill in the paleo-valley.

GPR SURVEYS ALONG ACTIVE TRACE OF KATROL HILL FAULT

Field evidence of lateral extension of surface faulting is presented in the previous chapter. GPR surveys were carried out along N-S transects (marked T3, T4, T5 and T6 in Figure 5.2) over the KHF zone with Quaternary sediment cover to delineate subsurface geophysical evidence of Late Quaternary surface faulting. The location of the GPR transects is marked in Figure 5.2. Although showing no deformational features in the field, the results of GPR at four sites clearly indicate the presence of tectonically induced deformation features and location of the KHF in the subsurface are presented in the following sub-

section. All the sites were selected based on neotectonic and geomorphic mapping of the KHF through and beyond the zones of observed fault exposures and DEM analysis.

Transect 3 – South of Bhujodi

This site (indicated as T3 in Figure 5.2) is located in the south of Bhujodi area near the northern flank of the Gangeshwar dome. A southerly oriented 50 m long GPR profile (Figure 6.4) was acquired across the ~W striking KHF. The reflections obtained from this site are categorized into various radar facies as shown in the interpreted profile (Figure 6.4c). The characteristics of radar signals signifying various radar facies Rf1–Rf7 are described below.

Aeolian miliolite deposits (Rf2 a–c): 0–5 m (0–80 ns) depth of the profile is occupied by cross-stratified aeolian miliolite deposits. Based on their geometry; Rf2 are sub-categorized into Rf2a, Rf2b and Rf2c (Figure 6.4c). Rf2 shows downlapping termination with unconformable contact and up-dip termination between 12–30 m distances. Towards the north, Rf2 is overlain by sub-horizontal, discontinuous reflections of Rf1 representing reworked miliolites deposits along the channel of the Gangeshwar river. Rf2a characterizes tabular, 8–15° north dipping cross-strata of aeolian miliolites. Based on the geometry and depositional pattern, Rf2a is interpreted to be representing the uppermost unit of the aeolian miliolite deposits. Between 18 and 30 m distances, facies Rf2b is observed with 25°–40° north dipping reflectors suggesting concave-up aeolian cross-strata (Figure 6.4c). Overall, the Rf2 facies correlates with the large scale aeolian cross stratification in the miliolite deposits lay down as obstacle dunes in the front of the north facing KHF scarps. Laterally, the facies Rf2b grades into deformed 41°–50° north dipping cross-strata of Rf2c. The unusually high dip of the cross strata correlates with the surface outcrops of aeolian miliolites in close vicinity that show sub-vertical beds along a narrow zone extending in E-W direction. The deformation of cross beds along a narrow zone suggests tectonic reactivation of the KHF in the subsurface after the depositional phase of miliolite sedimentation.

Erosional bounding surface: At ~4 m depth, Rf2a, Rf2b and Rf2c appears to downlap asymptotically to the unconformable erosional surface (Figure 6.4c). It is represented by 3°–5° south dipping continuous high-amplitude reflectors. The continuity of the reflections is lost in the hanging-wall of the KHF. They mark the eroded paleo-topography developed over the Jhuran and Bhuj sandstone in the subsurface.

Trough fills (Rf4): The trough fills are identified on the basis of the geometry of radar reflections Rf4. Between 33 and 47 m distances, Rf4 are observed in the hanging-wall

side of the KHF. Rf4 mainly comprises reflections from the subsequent filling of the erosional channel cuts indicating fluvial reworking of the aeolian miliolites (Figure 6.4b, c). The trough fills are attributed to minor shifts of the channel of Gangeshwar river presently located at the southern end of the GPR transect. The location of the site in front of the scarp indicating relatively unconfined nature of channel and along the KHF explains the minor channel shifts and fluvial dissection during the reworking of aeolian miliolite. Towards the southern side, the top portion comprising Rf3, which indicates prograding wedges, downlap onto Rf4. Rf5 characterizes reworked miliolite sediments, which occupy major portion of the hanging-wall of KHF. Rf6, the lowermost radar facies of Quaternary deposits, is characterized by wavy, semi-continuous reflections, which suggest stratified miliolites of gravelly nature.

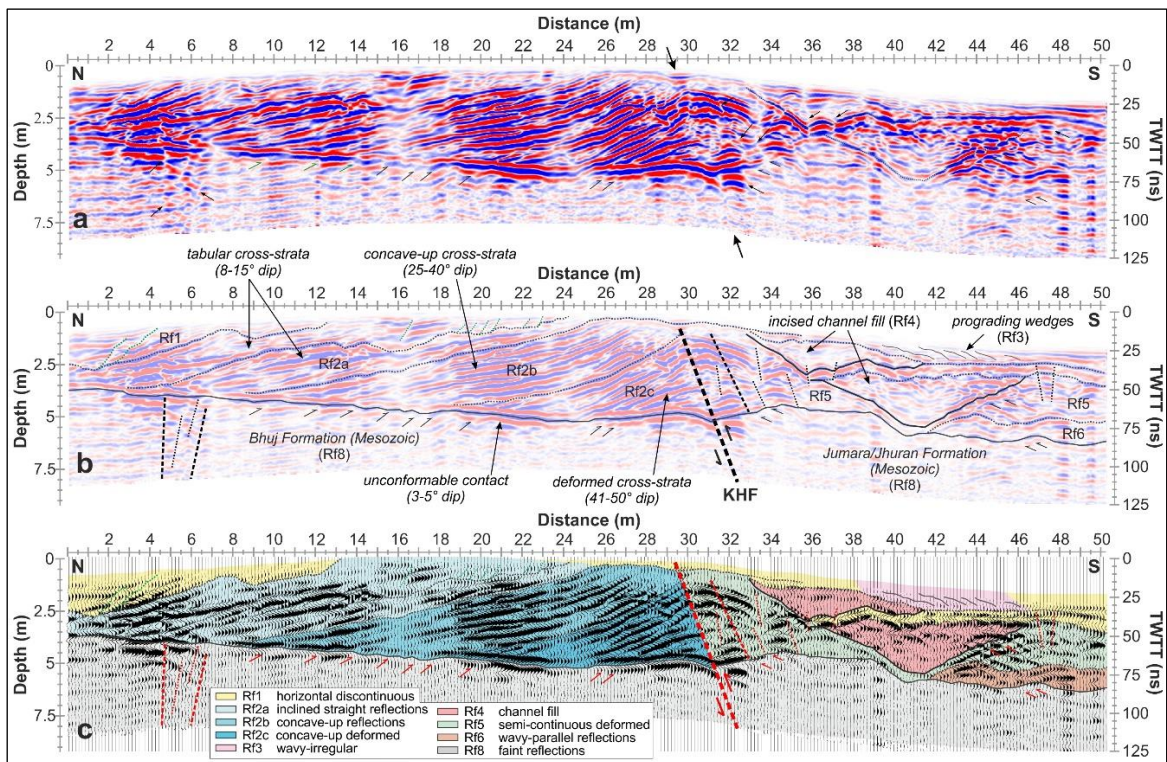


Figure 6.4 a. Processed GPR profile acquired from the Katrol Hill Fault (KHF) zone in front of the scarps. The general high amplitudes in the upper part of the radargram are from the Late Quaternary aeolian miliolite deposits overlying the fault line. **b.** Processed radargram showing the various radar facies, details of which are provided in Table 6.1. **c.** Interpreted radargram in wiggle format. Note the largely aeolian nature of the sediments reflected by the large-scale cross stratification. Also notice the high angle reverse nature of the KHF and its extension up to the surface offsetting the overlying sediment cover. The large scale aeolian cross stratification also gets markedly steeper along the fault plane. Note that the subsidiary antithetic and synthetic slip planes (marked by black and red dotted lines in Figures b and c, respectively) in the hanging-wall of KHF show a reverse slip-sense while those in the Mesozoic rocks in the footwall of KHF show a normal slip-sense.

Bhuj and Jhuran formations: The Late Quaternary miliolite deposits are underlain by the Bhuj Formation (sandstone) in footwall and Jhuran Formation (sandstone and shale) of Mesozoic age in the hanging-wall are represented by Rf8 in Figure 6.4c. These are characterized by low-amplitude, broken, chaotic reflections. The erosional truncation above Rf8 is clearly observed (marked by black arrows) at the unconformable contact with overlying miliolite sediments.

The position of the south dipping KHF in the subsurface at ~30 m distance and its reverse slip-sense is marked by: (i) abrupt termination of Rf2c concave-up cross-strata; (ii) 12°–18° south dipping strong amplitude reflections of Rf5 in the hanging-wall is in contrast to the 25°–40° north dipping reflections of Rf2c in the footwall (Figure 11c); truncation and dip change of the continuous reflectors of Rf2c and Rf5 is observed; (iii) reflectors of Rf5 are seen riding over the reflectors of Rf2c, meaning that the hanging-wall has moved up with respect to the footwall; note that no displacement is observed among these radar facies; and (iv) Older Jhuran Formation (Rf8) in the hanging-wall is in contact with the stratigraphically younger Bhuj Formation (Rf8) exposed in the footwall. However, it is to be noted that the displaced reflectors across the fault plane do not suggest the actual amount of displacement of the KHF. Moreover, the Late Quaternary neotectonic movement in the KHF deformation zone is further supported by: (i) the presence of subsidiary antithetic and synthetic faults in Quaternary sediments represented by Rf4, Rf5 and Rf6 and, (ii) the chaotic reflection pattern of Rf4 and the occurrence of erosional surfaces with scour and fill structures mainly at the upward (reverse) moving hanging wall of the KHF.

Transect 4 – Bharasar area

This site is located along a small north-flowing tributary of the Khari river to the north of the Bharasar dome (marked as T4 in Figure 5.2). The profile was acquired using 200 MHz antenna along NNW-SSE transect (Figure 6.5a, b). A sharp contrast in reflection pattern is noticed throughout the GPR profile near 60-70 ns (TWT) in Figure 6.5a, which separates the scattered low amplitude, discontinuous reflections of Mesozoic rocks at the lower section, overlain by high amplitude continuous reflections from the lithified Quaternary miliolite sediments towards the upper section of the radargram. A zone of slightly scattered and truncated radar reflectors in miliolite is seen at a distance of 15-25 m indicating deformation and offsetting of the reflections along a southward dipping fault plane of the KHF. The line drawing of this GPR profile (Figure 6.5b) demarcates the unconformable base between the Mesozoic and Quaternary sediments, erosional cut and fill

structures by younger sediments based on specific reflection pattern, amplitude variation and low angle dipping geometry of the fault plane. The deformation is traceable up to the bottom of the GPR profile in wiggle format (Figure 6.5a, b), is suggested by the continuity of reflectors along the fault plane. The interpretation of this zone suggests a south-dipping reverse nature of fault plane. Estimation of displacement along the fault plane is difficult to calculate due to poor continuity of reflectors at deeper intervals.

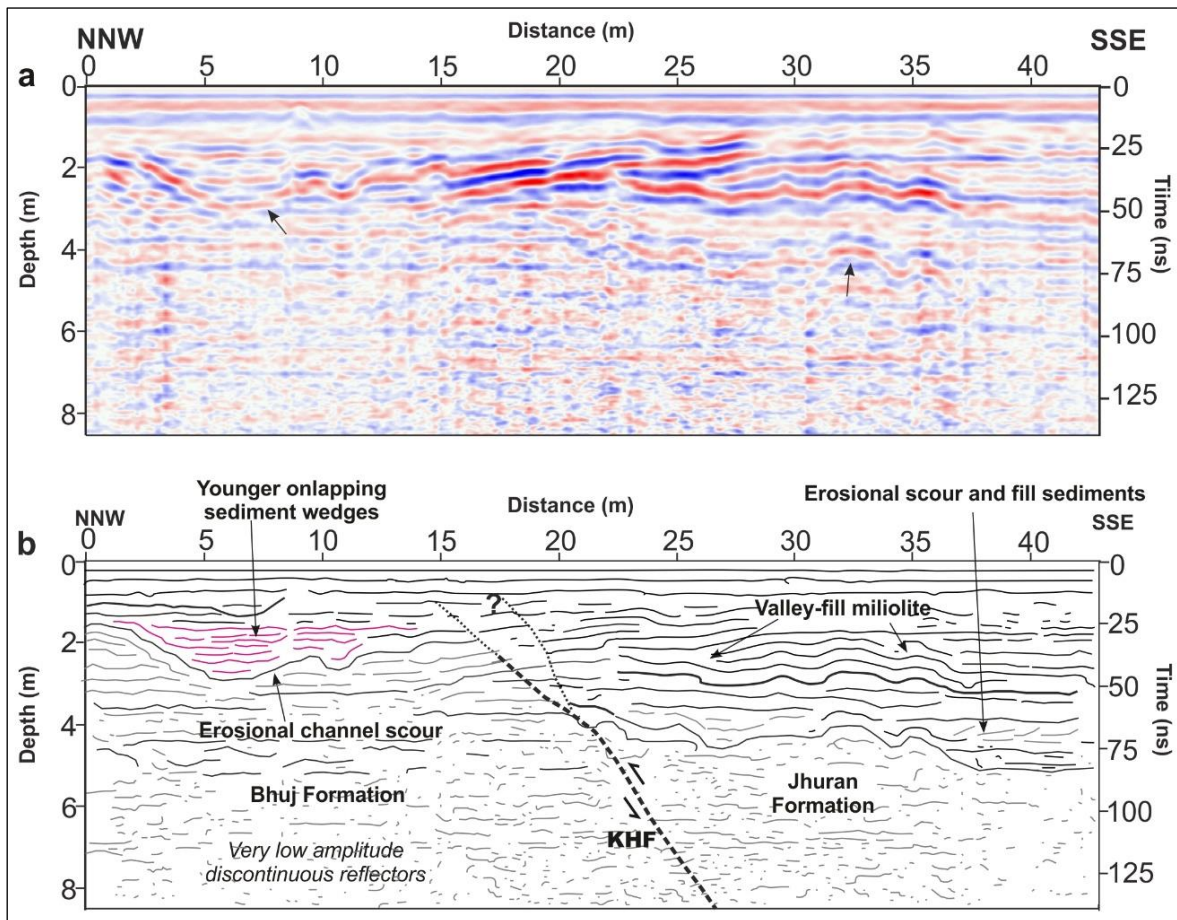


Figure 6.5 a. 200 MHz processed GPR profile in NNW-SSE direction acquired from south of Bharasar village. Arrows point to the onlapping wedge out and deformed geometry of near surface reflectors. The high amplitude continuous reflectors between 50 and 80 ns show erosional cut and fill geometries corresponding to the deposition of valley filled miliolite/younger sediments. **b.** Interpreted section of the GPR profile. The features are characterized on the basis of specific reflection pattern and amplitude variation. Note the changes in reflection pattern due to various geological features and reflectors offsetting along the fault plane.

The repetition of Quaternary sedimentary strata of similar physical properties makes it difficult to calculate the actual amount of offset along the fault plane in the GPR profile. The fault plane is dipping $\sim 50^\circ$ due south as seen in the GPR profile in overlaying Quaternary sediments, which is less than the dip of fault plane ($\sim 60^\circ$) in exposed Mesozoic

rocks at opposite bank of the stream. Wavy to discontinuous reflectors at the 4-7 m depth at a distance of 20-35 m of the GPR profile relate to the hanging wall sediment deformation during the inversion phase.

Transect 5 – Tapkeshwari area

This site is located to the south of Bhuj city on Bhuj-Tapkeshwari road (marked as T5 in Figure 5.2). The GPR profile is 45 m long and acquired along N-S oriented transect using 200 MHz frequency monostatic antenna (Figure 6.6a, b).

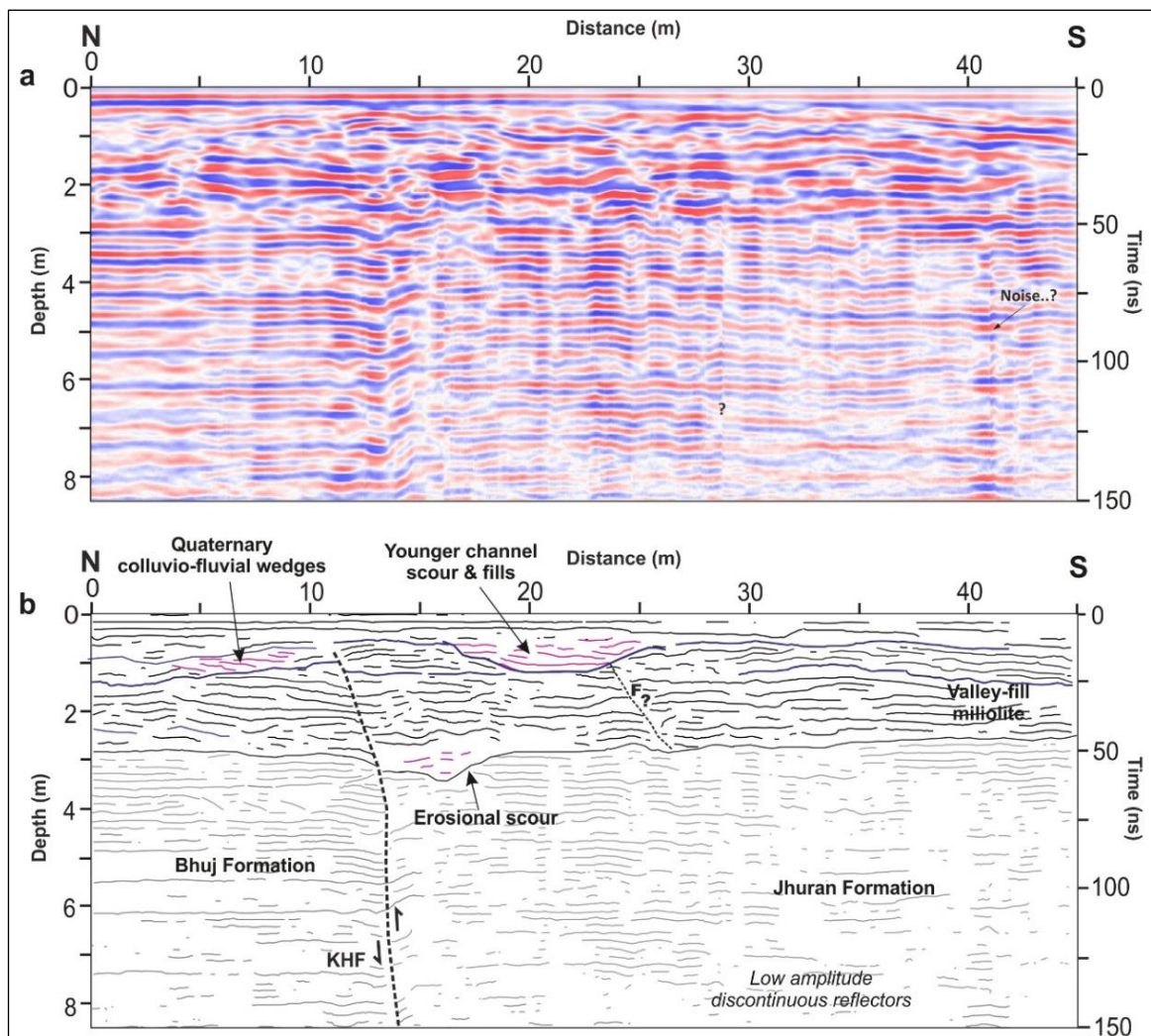


Figure 6.6 a. 200 MHz processed GPR profile in N-S direction obtained from Tapkeshwari area. **b.** Interpreted line drawing section based on GPR profile shown in a. Distinct changes in the reflector continuity and abrupt truncation along a plane is noticed between 10 and 15 m distance. The reflector offsetting, prograding colluvium wedges, younger channel cut and fill features are shown. The Quaternary-Mesozoic interface near 50–75 ns is marked based on reflector geometry/pattern and amplitude contrast. Based on deformed reflector and their abrupt truncation, the subsurface geometry of KHF is marked, which indicates gentle south dipping reverse fault plane that became almost vertical at depth.

Upper part of the radargram manifests distinct reflections with high amplitude and moderately continuous reflectors at up to ~50 ns. The onlapping wedge-out geometry is seen in the upper part of the profile (Figure 6.6b), which denotes erosional cut and fill sedimentary structures in the Late Quaternary fluvial deposits.

Based on the interpretation of reflection strength, geometry and amplitude contrast in GPR profile, the interface between Quaternary-Mesozoic formations is mapped at ~50 ns (Figure 6.6a, b). The strength of radar signal deteriorates slightly with depth due to changes in lithology and attenuation (Figure 6.6a). Abrupt changes in amplitude strength, signal scattering and reflection pattern observed across the fault plane corresponds to lithological variations. The horizontal, repetitive and abruptly truncating discontinuous reflectors around 13 m distance that characterize the fault plane in the radargram (Figure 6.6a, b).

Transect 6 – Ler area

This survey site is located near Ler village (marked as T6 in Figure 5.2) is the easternmost extremity of the ~21 kms length of the Late Quaternary surface faulting mapped in the present study. A 90 m long 200 MHz GPR profile was acquired in N-S direction across the inferred KHF fault trace is shown in Figure 6.7. Topographic corrections were applied using surface normalization function during processing to account for the uneven topography.

Offsetting along the fault plane is marked based on the contrasting amplitude patterns (Figure 6.7a, b). The comparatively continuous, thick and high amplitude reflection pattern towards the north of the GPR profile corresponds to the sandstone of Bhuj formation, while the low energy discontinuous reflections resemble the shales of Jhuran formation in the south part of the profile. The line drawing in Figure 6.7b shows distinct variations in the reflection pattern due to deformation and the Quaternary-Mesozoic interface around 3 m depth. The gently dipping KHF plane is interpreted at ~55 m distance characterized by reflector offsetting and abrupt truncation along a plane (Figure 6.7a, b).

The GPR data described above shows that the KHF propagated upwards into the overlying Late Quaternary sediments during the surface faulting events. Most of these evidences are from the miliolite sediments, suggesting that the post-miliolite surface faulting events, evident in the Khari river section (Figure 5.3) caused the KHF to rupture laterally. Petrographic and surface texture studies using SEM were carried out to further confirm and precisely estimate the length of Late Quaternary surface faulting along the KHF. Results from the GPR studies helped to choose precise locations for the collection of samples for petrographic and SEM studies to identify microscopic evidence of faulting.

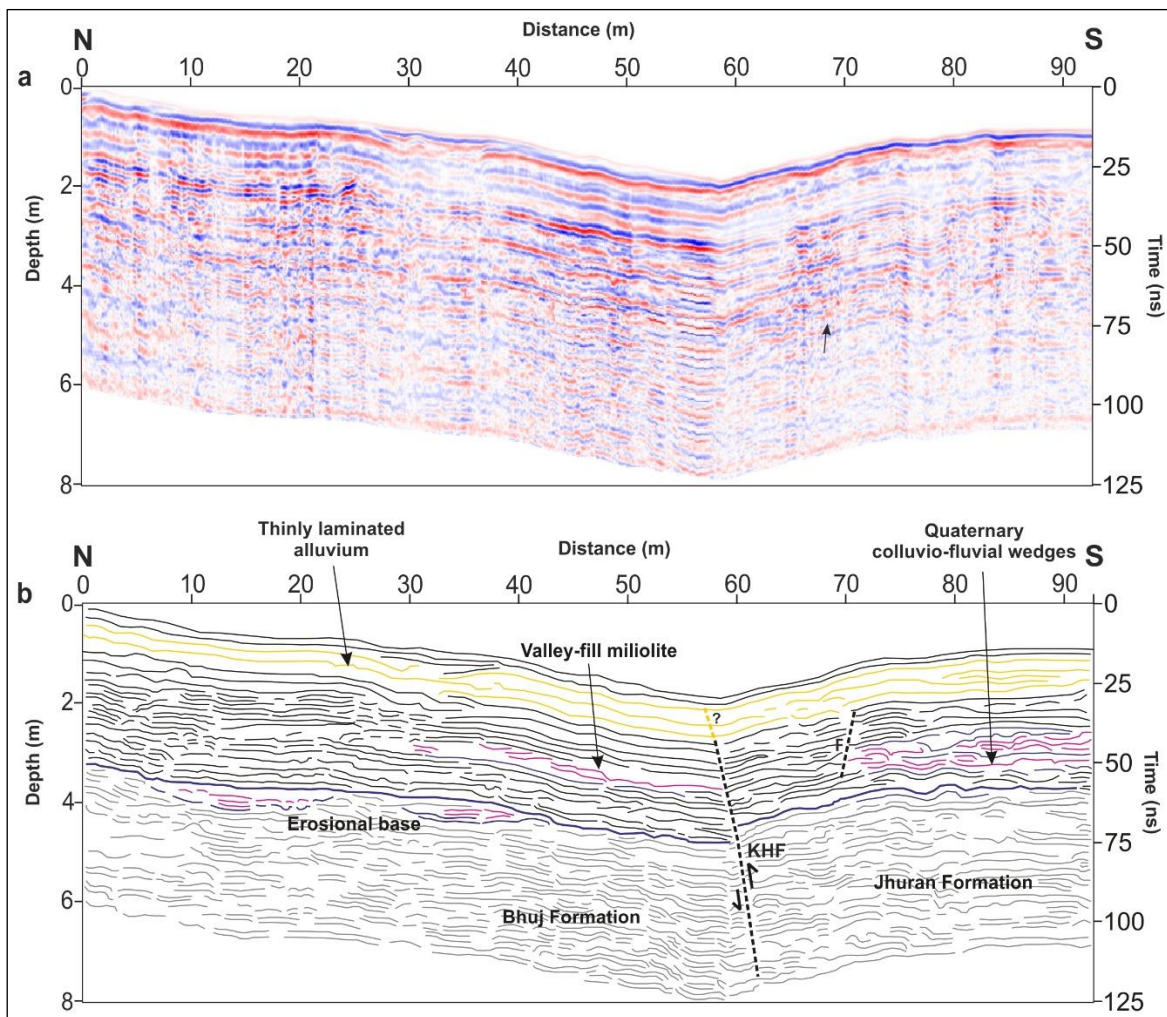


Figure 6.7 a. 200 MHz processed GPR profile in N-S direction obtained near Ler area. Note the offset and change in energy of reflectors across the fault plane (marked by dotted lines), which clearly depicts the changes in lithology; towards the north is the Bhuj formation showing continuous and high energy reflectors while the low energy discontinuous reflectors characterize the Jhuran formation. **b.** Interpreted line drawing section of GPR profile showing KHF plane based on reflector displacement and truncation along a plane. A distinct change in reflectors amplitude and presence of various deformational features in the upper section of the profile helps to define Quaternary-Mesozoic interface at ~50–60 ns. At ~25 ns it is difficult to outstretch the KHF plane up to the surface in profile due to highly rugged topography along GPR transect line and poor reflectivity from shallow section.